10.16920/jeet/2026/v39is4/26122

An Experiential Learning Framework for EV Charging Systems Using AI-Driven Harmonic Suppression and Advanced Quadrature Signal Generators

[1] C. R. Rajesh, [2]A. Bindu, [3]E. Jessy Mol, [4]C. Gnana Thilaka

[1,2]Department of Electrical and Electronics Engineering, CSI Institute of Technology, Thovalai, 629302, Tamilnadu, India

[3,4]Department of Electrical and Electronics Engineering, Ponjesly College of Engineering Nagercoil, 629003, Tamilnadu, India

[1]crrajesh99@gmail.com, [2]surabi74@gmail.com, [3]jessyjenkins2015@gmail.com, [4]thilakavibin@gmail.com

***Abstract*— With the growing use of fast Electric Vehicle (EV) charging systems, a set of complicated issues arises with regard to power quality, such as harmonic distortion, reactive power imbalance, and voltage instability. These obstacles necessitate sophisticated methods of control that in many cases students find hard to conceptualize on the basis of conventional modes of teaching. The research suggest an education-based framework that are incorporate the Model Predictive Control (MPC), the Wavelet Neural Networks (WNN), and the Quadrature Signal Generators (QSG) into a learning environment based on simulation in engineering. The suggested framework allows the students to comprehend the actual real-time problems of power quality with the help of interactive modeling and adaptive AI-mediated control methods. Two stage architecture is designed whereby the grid-side control is a finite-control-set MPC and adaptive control is a WNN-based controller. The system is instituted as a virtual laboratory module where the learners can see the harmonic suppression, reactive power compensation and power factor improvement. Education results show that students gain a better conceptual knowledge of the nonlinear systems, smart grid control, and AI-based optimization, and the analytical and problem-solving capabilities improve significantly. Multi-disciplinary learning is also supported by the framework across the boundaries of power electronics, artificial intelligence, and energy systems. The contribution to engineering education is that this work takes a complex real-life problem of EV charging control and makes it an interactive and student-focused learning experience, in accordance with the contemporary pedagogical principles like experiential learning and outcome-based learning.**

***Keywords*— Engineering Education; Experiential Learning; Simulation-Based Learning; EV Charging Systems; Power Quality Education**

I. INTRODUCTION

Electric mobility around the world has increased the pace of development of high frequency power electronic converters and fast EV charging stations that consume high amounts of power through the utility grid. These converters also have extremely nonlinear current waveforms unlike conventional linear loads, and introduce a lot of harmonic content into the distribution system. Subsequent power quality degradation is in the form of higher THD, lower power factor, distorted voltage, and possible resonant phenomena that negatively impact the grid infrastructure and co-located sensitive equipment(Çelik, 2025). Fast chargers, which are usually powered at the same level of current between 50 kW and more than 350 kW, use AC- DC rectification and then DC-DC conversion phases to supply controlled current to the battery. The AC-DC stage which is commonly a three phase SC is where the main source of harmonic injection is generated. The IEEE 519-2022 and IEC 61000-3-12 standards can be compromised by the low-order harmonics (5th, 7th, 11th, 13th) generated by six-pulse rectification without proper compensation. Besides, such harmonics under weak grid conditions with high source impedance lead to significant point-of-common-coupling (PCC) voltage distortion (Menos-Aikateriniadis, 2024).

The growing EVs has raised a new alarm over the issue of grid overloading due to the lack of coordination and simultaneous charge demand that require a sophisticated level of control and optimization measures. In response to this, a number of centralized and smart charging management methods have been suggested. The development of MPC can be regarded as a very effective method because of the possibility

C. R. Rajesh,
Department of Electrical and Electronics Engineering, CSI Institute of Technology, Thovalai
629302, Tamilnadu, India
crrajesh99@gmail.com

to predict system operation and optimize the charging processes in real-time considering grid limitations, electricity price levels, and customer preferences, which contributes to better demand-side management (DSM) and grid stability, (Wei, 2024). Simultaneously, multi-agent Deep Reinforcement Learning (DRL) and other data-driven methods of adaptive scheduling can be used in real time under unpredictable conditions to optimize the benefits of the user and the performance of the charging station (Fernandez, 2024). Further load balancing and cost reduction efforts are achieved by coordinated charging strategies; delayed charging, reduced-power charging, and Time-of-Use (ToU)-based smart charging with the ToU-based strategies demonstrating better results in re-shaping load profiles. Moreover, centralized schemes based on optimization by means of linear programming are helpful in the field of avoiding congestion and balancing between grid performance and user satisfaction (Li, 2025). Smart controllers, renewable energy (PV, wind, and battery storage) integration increase the efficiency of the system, the power quality, and its sustainability (Kundu, 2025).

Complicated methods, such as hybrid GA-ANN control and MPC-based station management show better charging efficiency, stability, and less error than traditional ones (Dreucci, 2025). In general, all these works indicate that predictive, optimization, and learning-based strategies need to be combined to create scalable, efficient, and user-friendly EV charging solutions and guarantee the effective grid functioning (El Ancary, 2025). The conventional passive filter-based compensation has resonance risk, constant tuning, and physical size. The Active Power Filters (APFs) enhance flexibility and are based on synchronization algorithms like Phase-Locked Loops (PLLs) and instantaneous power theory that are subject to performance degradation when there is deviation with the grid frequency and voltage unbalance. Moreover, the nature of conventional PI-based current regulators is also sensitive to changes in parameters and unable to handle the rapid transient nature of high-power EV chargers (Watil, 2024). Model Predictive Control (MPC) has been practically applied in power converters, due to the availability of advanced digital signal processors and field-programmable gate arrays. Finite-Control-Set MPC (FCS-MPC) is an approach that directly takes advantage of the discrete nature of the converter switching, and compares a finite number of switching states to reach the optimal action that optimizes a cost model. This allows it to do away with the modulation stages and provides rapid dynamic response, the inherent multi-objective optimization ability, and simple integration of system constraints. At the same time, artificial intelligence methods especially neural networks have shown impressive ability of approximating nonlinear mappings that are complex. Wavelet Neural Networks (WNNs): Wavelet basis functions possess the ability to localize, which is combined with neural networks, which have the ability to generalize. The time-varying nature of battery terminal voltage and charge profiles is highly FF which is why wavelets are especially suited to transient features allowing adaptive control mechanisms to be applied which traditional neural networks cannot achieve because of their multi-resolution properties. Quadrature Signal Generators (QSGs), particularly Second-Order Generalized Integrators (SOGIs) offer precise orthogonal pairs of signals to do frequency-adaptive grid synchronization that do not suffer the latency and sensitivity challenges of the traditional PLLs. By combining QSG-based synchronization with MPC and WNN control architectures, it is possible to establish a synergistic framework that can safely be used in a large variety of grid conditions.

This research has the following original contributions:

- Development of a simulation-based learning module for EV charging systems using MPC and WNN
- Integration of AI-driven adaptive control concepts into engineering curriculum
- Design of a virtual lab environment for harmonic analysis and reactive power compensation
- Implementation of student-centered learning using real-world case studies
- Assessment framework to evaluate learning outcomes in smart grid technologies

II. Proposed Methodology

The EV fast charging system proposed is a three-principal subsystem in Fig. 1, including (1) three phase grid interface, which includes a VSC with LCL filter, (2) isolated DC-DC converter stage, and (3) Battery Management System (BMS). The two stage control platform has FCS-MPC at the AC-DC level and WNN adaptive control at the DC-DC level, with the SOGI-QSG synchronization module integrating them. These modules are designed to help students understand the interaction between power electronic subsystems in real-world EV charging applications. The control architecture is presented as a two-stage learning model, where Finite Control Set Model Predictive Control (FCS-MPC) is implemented at the AC–DC stage to demonstrate grid-side control concepts such as current tracking, harmonic suppression, and reactive power compensation.

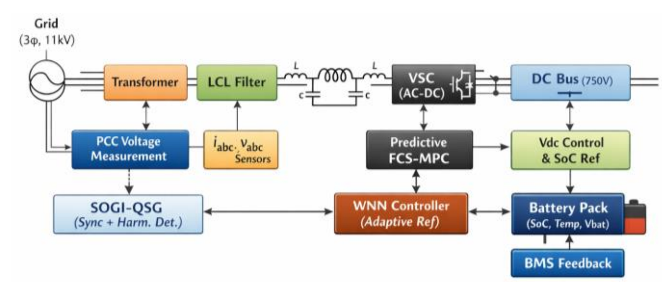

Fig. 1. Proposed SOGI-QSG with WNN controller Model

A. Grid-Side VSC Model

The 3-phase VSC, connected with AC grid via an LCL filter, is modeled in the synchronous rotating reference frame (d–q frame) with angular frequency ω. The dynamic equations governing the converter and grid side currents are given as follows:

$$L_1 \frac{di_{cd}}{dt} = v_{cd} - v_{fd} - R_1 i_{cd} + \omega L_1 i_{cq} \tag{1}$$

$$L_1 \frac{di_{cq}}{dt} = v_{cq} - v_{fq} - R_1 i_{cq} + \omega L_1 i_{cd} \quad (2)$$
$$L_2 \frac{di_{gd}}{dt} = v_{fd} - v_{gd} - R_2 i_{gd} + \omega L_2 i_{gq} \quad (3)$$
$$L_2 \frac{di_{gq}}{dt} = v_{fq} - v_{gq} - R_2 i_{gq} + \omega L_2 i_{gd} \quad (4)$$

where L_1, R_1 denotes the inductance and resistance of converter side, and L_2, R_2 represents the inductance and resistance of grid area. The variables v_{cd} and v_{cq} denotes converter output voltages, v_{fd} and v_{fq} signifies filter capacitor voltages, and v_{gd} and v_{gq} implies grid voltages expressed in the d–q frame.

The filter capacitor voltage dynamics are described by:

$$C_f \frac{dv_{fd}}{dt} = i_{cd} - i_{gd} + \omega C_f v_{fq} \quad (5)$$
$$C_f \frac{dv_{fq}}{dt} = i_{cq} - i_{gq} + \omega C_f v_{fd} \quad (6)$$

The instantaneous active and reactive power injected into the grid, assuming d-axis alignment with the grid voltage vector ($v_{gq} = 0, v_{gd} = V_g$), as given in Eq. (7)

$$P = 3/2\, v_{gd} i_{gd}; \quad Q = -3/2 v_{gd} i_{gq} \quad (7)$$

The q-axis current i_{gq} is regulated to zero in order to ensure unity power factor operating, and the d-axis current i_{gd} is managed in accordance with the DC-link voltage regulation and the power needs for EV charging.

1) DC-Link Voltage Dynamics

The term V_{dc} as DC-link capacitor voltage is directed by the power balance among the VSC of grid side and the DC–DC converter interfacing the EV load:

$$C_{dc} \frac{dV_{dc}}{dt} = i_{dc,VSC} - i_{dc,load} = \frac{P_{grid}}{V_{dc}} - \frac{P_{EV}}{V_{dc}} \quad (8)$$

Here C_{dc} indicates capacitance of DC-link, $i_{dc,vsc}$ is the current supplied by the VSC, and $i_{dc,load}$ represents current drawn by the EV-side converter. Proper regulation of V_{dc} is essential to maintain system stability and avoid overvoltage or undervoltage conditions on the DC bus.

2) Battery Model

The lithium-ion battery is modeled using a Thevenin equivalent circuit, which effectively captures its dynamic behavior:

$$V_{bat} = V_{oc}(soc) - R_0 i_{bat} - V_{RC} \quad (9)$$
$$C_P \frac{dV_{RC}}{dt} = i_{bat} - \frac{V_{RC}}{R_P} \quad (10)$$

Here $V_{oc}(soc)$ represents open-circuit voltage as a nonlinear function of the SoC, R_0 implies internal resistance, and R_P and C_P indicates the polarization resistance and capacitance, respectively. V_{RC} denotes the voltage across the RC branch, capturing transient electrochemical effects.

The SOC is estimated using the Coulomb counting method:

$$soc(t) = soc(0) - \frac{1}{Q_n}\int_0^t i_{bat}(\tau)d\tau \quad (11)$$

where Q_n is the nominal battery capacity (Ah).

B. SOGI-QSG synchronization and Harmonic Detection

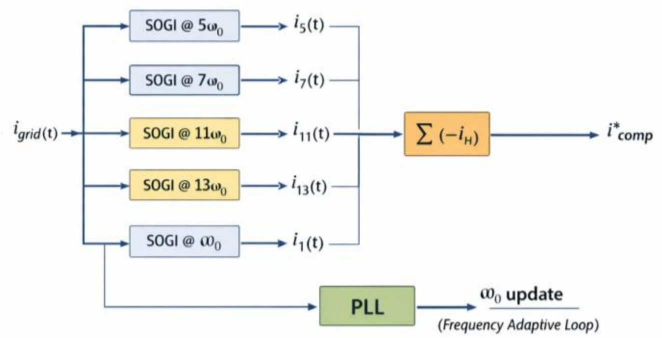

Fig. 2. SOGI-QSG Multi harmonic detection architecture

Fig. 2 shows the structure of SOGI-QSG Multi harmonic detection. The SOGI is used to generate orthogonal signals for grid synchronization. Its transfer function are given by,

$$D(s) = \frac{k\omega_0 s}{s^2 + k\omega_0 s + \omega_0^2}, \; Q(s) = \frac{k\omega_0^2}{s^2 + k\omega_0 s + \omega_0^2} \quad (12)$$

Where $k = \sqrt{2}$ ensures optimal damping. A phase-Locked Loop (PLL) adapts the frequency using,

$$\varepsilon_{PLL} = \frac{v'_\alpha \cdot q v'_\alpha}{|v'_\alpha|}, \quad \omega_0(s) = \left(k_p + \frac{k_i}{s}\right)\varepsilon_{PLL}(s) \quad (13)$$

For harmonic extraction, multiple SOGI units tuned at $\omega_h = h\omega_0$ are used,

$$i_h(t) = D_h(j\omega_h) i_{grid}(t), i^*_{comp}(t) = -\sum_{h\in\{5,7,11,13\}} i_h(t) \quad (14)$$

C. Finite Control-Set Model Predictive Control

The discretized system can be given in Eq. (15)

$$x[k+1] = A_d x[k] + B_d u[k] + E_d w[k] \quad (15)$$

The 2-step prediction is applied to address computation delay as,

$$x[k+2] = A_d x[k+1] + B_d u_j + E_d w[k] \quad (16)$$

The multi-objective cost function is defined as,

$$J = \lambda_1 |i^*_{gd} - i_{gd}|^2 + \lambda_2 |i^*_{gq} - i_{gq}|^2 + \lambda_3 (V^*_{DC} - v_{DC})^2 + \lambda_4 n_{sw} + \lambda_5 THD^2_{est} \quad (17)$$

Where the total THD is estimated by Eq. (18),

$$THD_{est} = \frac{\sqrt{\sum_{h=2}^{N} I_h^2}}{I_1} \times 100\% \quad (18)$$

This enables optimal current tracking, harmonic mitigation and efficient switching with improved grid power quality.

1) Optimal Switching State Selection

At each sampling instant k, the cost function is estimated for switching states, and the optimal voltage vector is selected as:

$$u^*[k] = arg \min_{u_j \in \Omega_u} J(u_j) \quad (19)$$

The selected state is directly applied to the VSC without PWM, resulting in variable switching frequency operation. The switching frequency is indirectly controlled by the penalty term λ_4, and the algorithm is executed within a sampling period of $T_s = 100\,\mu_s$.

III. Wavelet Neural Network Adaptive Controller

The WNN employs a three-layer architecture with Morlet wavelet activation functions to capture nonlinear battery dynamics (Esen, 2011). Fig. 3 illustrates the WNN control modelling.

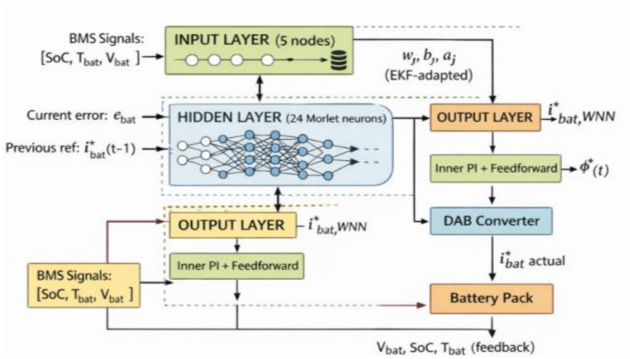

Fig. 3. Modelling of WNN adaptive control structure

The input vector is:

$$x_{WNN} = [soc, T_{bat}, V_{bat}, i^*_{bat}, e_{bat}]^T \quad (20)$$

The hidden neuron output is described in Eq. (21)

$$\psi_j(x) = \cos(1.75\zeta_j e^{\frac{-\zeta_j^2}{2}}; \quad \zeta_j = \frac{w_j^T x - b_j}{a_j}) \quad (21)$$

The WNN output (charging current reference) is:

$$i^*_{bat,WNN}(t) = \sum_{j=1}^{N_w} c_j \psi_j(x_{WNN}) \quad (22)$$

The WNN parameters are updated online using the Extended Kalman Filter.

A. DC–DC Converter Integration

A bidirectional Dual Active Bridge (DAB) converter regulates power transfer using phase-shift control towards battery.

$$P_{DAB} = \frac{V_{dc}V_{bat}\phi(1-|\phi|/\pi)}{2\pi f_{sw}L_r} \quad (23)$$

The control law combines feedback and WNN feedforward compensation:

$$\phi^*(t) = k_p^{DAB}\left(i^*_{bat,WNN} - i_{bat}\right) + \phi_{WNN,FF} \quad (24)$$

IV. Results And Discussion

A. Simulation Setup

The suggested control structure was tested and confirmed on MATLAB/Simulink R2021b. Table I includes the parameter of the system. The simulation involves five test conditions, i.e. (1) steady-state strong grids operation, (2) abrupt half to full rated power load step, (3) weak grid (X/R = 5, SCR = 5), (4) nonlinear load perturbation, (5) battery SoC perturbation between 20 and 90%. The proposed FCS-MPC +WNN architecture is compared to three benchmarks: traditional PI control (PI), traditional FCS-MPC using no harmonic terms (MPC-STD), and independent Back propagation Neural Network (BPNN) controller.

TABLE I
System Parameters

Parameter	Symbol	Value
Grid Phase Voltage	v_g	230V
Grid Frequency	f_o	50Hz
DC-Link Voltage Reference	v^*_{dc}	750V
Inductance	L_1	3.2mH
Inductance	L_2	0.8mH
Filter Capacitance	C_f	$25\mu_F$
DC-Link Capacitance	C_{dc}	$4700\mu_F$
Sampling / Control Period	T_s	$100\mu_s$
Rated Charging Power	P_{EV}	150kW
Battery Nominal Voltage	$V_{bat,nom}$	400V
Battery Capacity	Q_n	100Ah
DAB Switching Frequency	f_{sw}	10kHz
WNN Hidden Neurons	N_w	24
SOGI Damping Factor	k	1.414 (√2)

B. Steady-State Harmonic Performance

With an inflexible grid (SCR = 20) under rated power conditions, the proposed framework demonstrates a THD of 2.7% in the current in the grid-side, well below the IEEE standard of 5% in systems over 100 kVA. Fig. 4 illustrates the grid current waveform and its harmonic spectrum. Table II shows the THD comparative performance analysis.

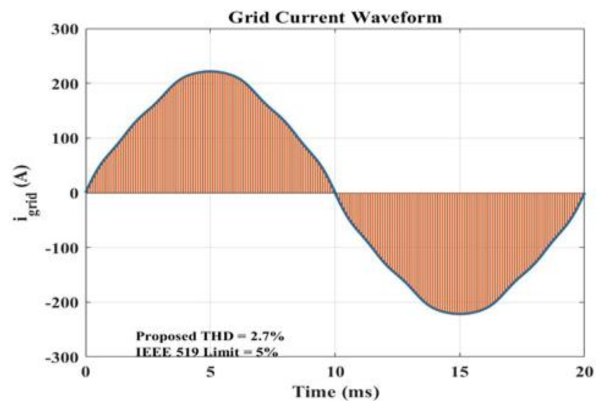

a)

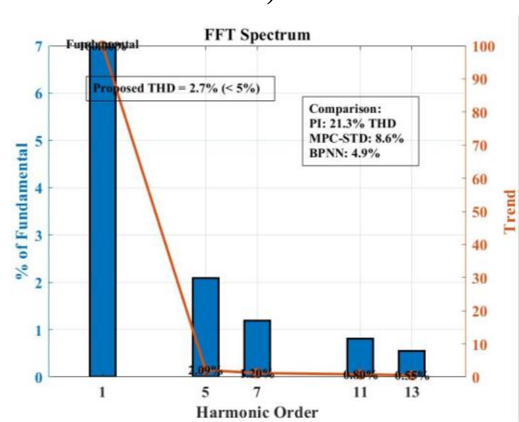

Fig. 4: a) Grid current waveform and b) FFT Spectrum

C. Dynamic Response to Load Step

A 100% load step (from 75 kW to 150 kW) is applied at t = 0.3 s. Fig. 5 shows the DC-link voltage transient response for all four control strategies. The proposed FCS-MPC+WNN achieves a settling time of 7.8 ms with a maximum voltage undershoot of 12 V (1.6%). In contrast, the PI controller exhibits a settling time of 48 ms with a 43 V (5.7%) undershoot, while MPC-STD and BPNN achieve settling times of 18 ms and 22 ms, respectively.

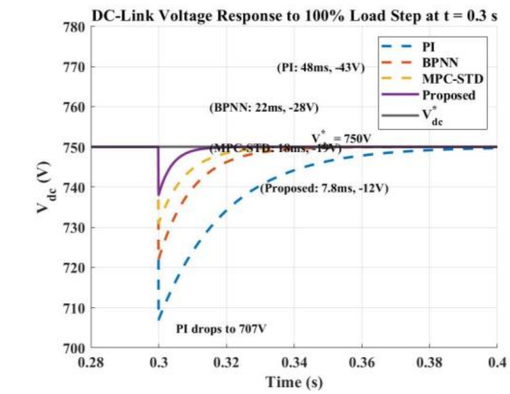

Fig. 5. DC link voltage response

D. Battery Charging Performance

The WNN adaptive controller is evaluated over a complete constant-current (CC) to constant-voltage (CV) charging cycle from SoC = 20% to SoC = 90%. Fig. 6 illustrates the charging current reference tracking and the SoC profile.

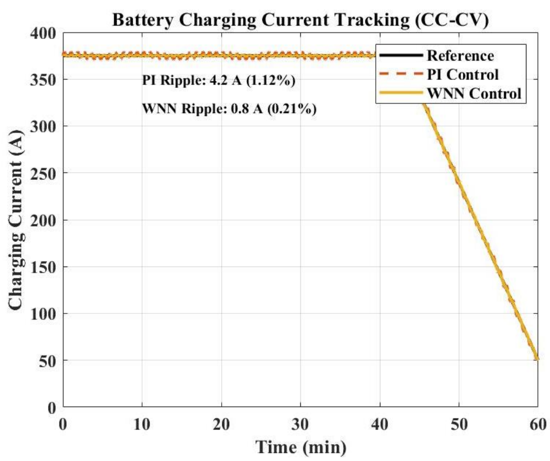

a)

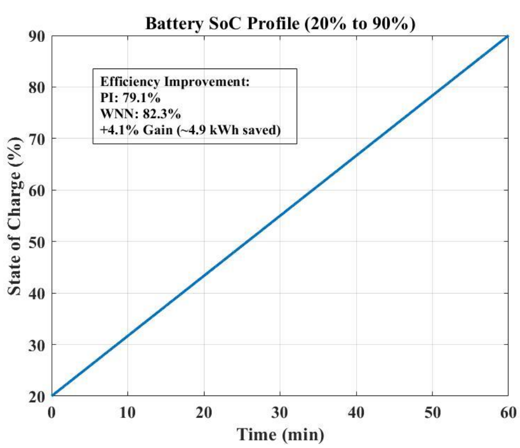

b)

Fig. 6. a) Battery charging current tracking and b) Battery SOC

The WNN controller achieves a charging current ripple of 0.8 A RMS (0.21% of rated 375 A), compared to 4.2 A RMS (1.12%) for PI control. The charging efficiency, defined as the ratio of energy stored in the battery to energy drawn from the DC bus, improves from 79.1% (PI) to 82.3% (WNN), a 4.1% absolute improvement that translates to approximately 4.9 kWh saved per full charging cycle for a 100 Ah/400 V battery.

E. Weak Grid Performance

Under weak grid conditions (Short Circuit Ratio SCR = 5, X/R = 5), grid impedance causes significant voltage distortion at the PCC. As shown in Table II, the proposed method limits current THD to 3.8%, while the PI controller's THD rises to 28.4% and even MPC-STD deteriorates to 14.3% due to lack of harmonic-aware cost function terms. The reactive power deviation under weak grid with sudden reactive load injection (100 kVAR at t = 0.5 s) is limited to ±2.3 kVAR by the proposed controller, compared to ±18.7 kVAR for PI control, demonstrating superior reactive power compensation capability.

TABLE II
THD COMPARISON UNDER DIFFERENT OPERATING CONDITIONS

Control Strategy	THD at 100% Load (%)	THD at 50% Load (%)	THD (Weak Grid, SCR=5) (%)	Power Factor
Conventional PI	21.3	18.7	28.4	0.86
MPC-Standard	8.6	7.2	14.3	0.93
BPNN Controller	4.9	4.1	9.7	0.97
Proposed FCS-MPC+WNN	2.7	2.1	3.8	0.991
IEEE 519-2022 Limit	5.0	5.0	5.0	≥0.95

F. Power Factor and Reactive Power Compensation

Table III summarizes the power quality metrics achieved by the proposed framework across all test scenarios. The near-unity power factor of 0.991 is maintained robustly across load variations from 20% to 100% of rated power, and across grid SCR values from 5 to 20. The reactive power compensation error remains below 2.5 kVAR in all tested conditions.

TABLE III
COMPREHENSIVE POWER QUALITY METRICS FOR PROPOSED FCS-MPC+WNN

Operating Condition	THD (%)	Power Factor	Q Error (kVAR)	V_dc Settling (ms)	Charging η (%)
Rated Load, Strong Grid	2.7	0.991	1.2	7.8	82.3
50% Load, Strong Grid	2.1	0.994	0.8	6.4	83.7
20% Load, Strong Grid	3.4	0.989	1.5	9.1	80.2
Rated Load, Weak Grid (SCR=5)	3.8	0.987	2.3	11.2	81.8
Load Step (50%→100%)	3.1	0.988	2.1	7.8	—
Nonlinear Load Perturbation	3.6	0.986	2.5	13.5	—
Temperature Stress (45°C)	2.9	0.990	1.4	8.3	81.5

Figure 7 presents comparison of all four control strategies across four performance dimensions: THD, power factor, weak grid robustness, and charging efficiency. The key advantage relative to MPC-STD lies in the harmonic-aware cost function and SOGI-QSG integration, which provide a 68.6% THD reduction compared to MPC-STD's 59.6% reduction versus PI.

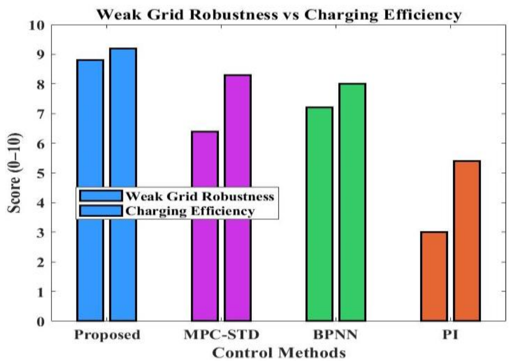

a)

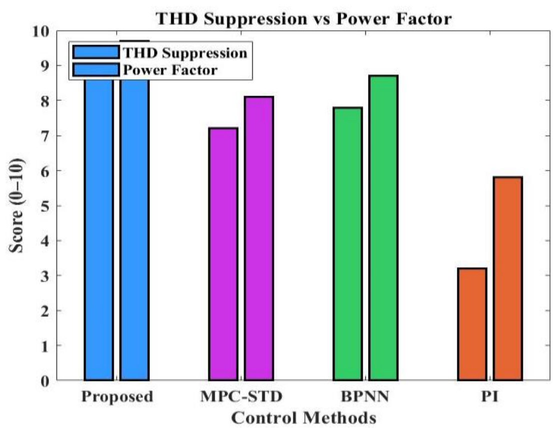

b)

Fig. 7. comparative analysis of a) Robustness and charging efficiency and b) THD suppression and power factor

The modular structure of the framework supports progressive learning, where students first understand fundamental concepts and then gradually move toward complex system-level interactions. The inclusion of real-world EV charging scenarios enhances contextual learning, making the subject more relevant and engaging. Student activities reveal that learners develop:

- Improved analytical skills through performance evaluation
- Enhanced problem-solving ability via controller design
- Better interdisciplinary understanding combining AI and power systems

Furthermore, the use of SOGI-QSG for synchronization introduces learners to advanced signal processing techniques, which are often difficult to grasp through theoretical instruction alone.

V. Conclusion

In this work, an education-focused transformation of a sophisticated EV fast charging control system into a learning framework with simulation is introduced. The proposed approach combines MPC, WNN and QSG, allowing students to learn the complex issue of power quality through an interactive, intuitively-designed approach. The framework is successful in filling in the gap between theory and practice, and enhances deeper insight about smart grid technologies. The methodology improves student engagement, conceptual clarity, and interdisciplinary learning through structured student activities and performance-based assessment. The findings reveal that the integration of AI-controlled strategies into engineering training can have a beneficial impact on the skills of students in the analysis and design of contemporary energy systems. The practice is in line with the current trends in transforming engineering education which have focused on experiential learning, digital simulation and solving real life problems. The next-generation work can further evolve this framework to hardware-in-the-loop (HIL) systems and remote laboratories, which will further reinforce a more practical exposure and industry preparedness.

References

Çelik, D., Khan, M. A., Khosravi, N., Waseem, M., & Ahmed, H. (2025). A review of energy storage systems for facilitating large-scale EV charger integration in electric power grid. Journal of Energy Storage, 112, 115496.

Dreucci, D., Yu, Y., Mouli, G. R. C., Shekhar, A., & Bauer, P. (2025). Centralised distribution grid congestion management through EV charging control considering fairness and priority. Applied Energy, 384, 125417.

El Ancary, M., Lassioui, A., El Fadil, H., El Asri, Y., Hasni, A., & Nady, S. (2025). Design and experimental validation of wireless electric vehicle charger control using genetic algorithms and feedforward artificial neural network. Eng, 6(3), 43.

Esen, H., Ozgen, F., Esen, M., & Sengur, A. (2009). Artificial neural network and wavelet neural network approaches for modelling of a solar air heater. Expert Systems with Applications, 36(8), 11240–11248.

Fernandez, V., & Pérez, V. (2024). Optimization of electric vehicle charging control in a demand-side management context: A model predictive control approach. Applied Sciences, 14(19), 8736.

Kundu, S., Singh, M., Giri, A. K., Kadiyan, S., Chittora, P., & Shailly, D. (2025). Robust and fast control approach for islanded microgrid system and EV charging station applications. Electrical Engineering, 107(7), 8385–8396.

Li, Y., Zhang, Z., & Xing, Q. (2025). Real-time online charging control of electric vehicle charging station based on a multi-agent deep reinforcement learning. Energy, 319, 135095.

Menos-Aikateriniadis, C., Sykiotis, S., & Georgilakis, P. S. (2024). Unlocking the potential of smart EV charging: A user-oriented control system based on deep reinforcement learning. Electric Power Systems Research, 230, 110255.

Watil, A., & Chojaa, H. (2024). Enhancing grid-connected PV–EV charging station performance through real-time dynamic power management using model predictive control. Results in Engineering, 24, 103192.

Wei, H., Wu, J., Lv, C., Yang, S., Zhang, H., & Al-Haddad, K. (2024). Intelligent EV charging control and management: From microscale battery cell to macroscale grid synergy. IEEE Transactions on Intelligent Vehicles.